Available online at www.sciencedirect.com
SCIENCE DIRECT®
Journal of Solid State Chemistry 179 (2006) 205–211
JOURNAL OF SOLID STATE CHEMISTRY
www.elsevier.com/locate/jssc

The actual structure of $K_6(VO)_2(V_2O_3)_2(PO_4)_4(P_2O_7)$: Ordered distribution of P_2O_7 groups and charge ordering of vanadium

A. Leclaire*, B. Raveau

Laboratoire CRISMAT, UMR CNRS ENSICAEN 6508, 6 bd Maréchal Juin, 14050 CAEN Cedex 4, France

Received 4 July 2005; received in revised form 6 October 2005; accepted 16 October 2005
Available online 15 November 2005

Abstract

The actual structure of the vanadium phosphate $K_6(VO)_2(V_2O_3)_2(PO_4)_4(P_2O_7)$ has been determined, using a much larger single crystal than previously used for the isostructural Rb-phase. The actual supercell is four times larger than the corresponding orthorhombic subcell with $a = 26.777$ Å, $b = 28.480$ Å, $c = 6.972$ Å, $\alpha = \beta = \gamma = 90^\circ$. The structure resolution, performed in the triclinic space group C-1, shows that the P_2O_7 groups alone are responsible for the superstructure, all the other atoms keeping the atomic positions of the orthorhombic subcell. This structural study shows a perfect ordering of the P_2O_7 groups in the actual structure, in contrast to the results obtained from the subcell. Concomitantly, the V^{4+} and V^{5+} are found to be ordered in the form of [110] stripes.

Keywords: Potassium vanadium phosphates; Monophosphates mixed to diphosphates; Actual structure; Mixed V^{4+}/V^{5+} vanadium phosphate; Charge ordering of vanadium; Ordered frameworks

1. Introduction

Mixed valent transition metal phosphates form a large family of mixed frameworks built up from PO_4 tetrahedra and transition metal polyhedra, i.e. MO_6 octahedra, or MO_5 pyramids or MO_4 tetrahedra. In these compounds, the strong covalency of phosphorus makes such mixed frameworks generally well ordered, leaving only a possibility of charge order–disorder phenomena of the transition elements in their polyhedra. For instance, in the tungsten phosphate bronzes [1] the monophosphate or diphosphate groups and the WO_6 octahedra form a very well ordered array, whereas the tungsten charge is disordered, corresponding to a complete electronic delocalization so that metallic conductivity and charge density wave properties are observed [2]. For the mixed valent molybdenum and vanadium phosphates [3], the phosphate groups and the VO_n or MoO_n polyhedra also form a generally well ordered framework, but the electronic delocalization in those systems is rather rare so that charge ordering is often observed.

The studies of the vanadophosphates $Rb_6(VO)_2(V_2O_3)_2(PO_4)_4(P_2O_7)$ [4] and $A_6(V_2O_3)_2(VO)_2(PO_4)_4(H_yP_{2-x}V_xO_7)$ with $A = K$, Rb, Tl [5,6] showed a quite unusual disordered distribution of the P_2O_7 groups in the mixed frameworks of this series of isostructural compounds. Similarly, a disordered distribution of PO_4 tetrahedra was previously observed for the phosphate $Mo_2P_4O_{15}$ [7], but the redetermination of the crystal structure of the latter, 12 years later by Lister et al. [8], using a much larger crystal, allowed much weaker superstructure reflections to be detected, leading to a huge supercell, 21 times larger than the initial one. As a consequence, the corresponding structure determination demonstrated, that in fact the PO_4 tetrahedra were perfectly ordered. Bearing in mind the latter results, we have tried to grow larger crystals of $A_6(VO)_2(V_2O_3)_2(PO_4)_4(P_2O_7)$ for $A = K$, Rb in view of a structure redetermination. These attempts were successful for the potassium phosphate, $K_6(VO)_2(V_2O_3)_2(PO_4)_4(P_2O_7)$, allowing a single crystal ten times larger than for the Rb-phase [4] to be isolated. We report herein on the structure redetermination of this structural type. We show

*Corresponding author. Fax: +33 2 31 95 16 00.
E-mail address: andre.leclaire@ensicaen.fr (A. Leclaire).

0022-4596/$ - see front matter © 2005 Elsevier Inc. All rights reserved.
doi:10.1016/j.jssc.2005.10.013

that this phosphate exhibits a surpercell, four times larger than initially found for the Rb-phase, and that the diphosphate groups are in fact perfectly ordered in the framework of the actual structure. Moreover, bond valence sum calculations evidence a perfect ordering of the V^{4+} and V^{5+} species, in contrast to what was found previously for a much smaller crystal of the Rb phosphate.

Table 1
Summary of crystal data, intensity measurement, and structure refinement for the subcell and the supercell of $K_6(VO)_2(V_2O_3)_2(PO_4)_4(P_2O_7)$

	Subcell	Supercell
Chemical formula	$K_6V_6P_6O_{31}$	$K_6V_6P_6O_{31}$
Space group	*Pnma*	*C*-1
a (Å)	6.9801(9)	26.7777(5)
b (Å)	13.389(3)	28.4800(5)
c (Å)	14.235(2)	6.9762(5)
α (deg)	90	90
β (deg)	90	90
γ (deg)	90	90
V (Å^3)	1330.3(3)	5320.2(2)
Z	2	8
Molecular weight (Da)	1222.05	1222.05
Density (g cm^{-3})	3.050	3.050
Linear absorption (mm^{-1})	3.453	3.453
T_{min}	0.9100	0.8086
T_{max}	0.9443	0.9056
Crystal size (mm)	$0.044 \times 0.033 \times 0.032$	$0.087 \times 0.069 \times 0.037$
Crystal volume (mm^3)	0.00001878	0.00012231
Number of measurement	11 376	26 714
Number of $I \geqslant 3\sigma(I)$	5474	12 144
Number of independent *h k l* with $I \geqslant 3\sigma(I)$	1328	5307
Refined parameters	130	547
R (%)	4.67	5.06
R_w (%)	3.17	5.12
σ/Δ	0.0004	0.02

1.1. Crystal growth

Single crystals suitable for X-ray diffraction studies were isolated from a batch of nominal composition $K_2V_2P_2O_{11}$. First K_2CO_3, $H(NH_4)_2PO_4$ and V_2O_5 were mixed in an agate mortar in the molar ratio 1:2:1 and heated at 673 K in a platinum crucible to decompose the ammonium phosphate and the carbonate. In a second step the resulting mixture added to KCl (0.06) was crushed in an agate mortar and sealed in an evacuated silica ampoule. The latter was then heated for 1 day at 923 K, cooled at 4 K/h down to 473 K and finally quenched to room temperature. From the resulting product two kinds of well formed crystals were extracted: green crystals of $K_2VO(P_2O_7)$ [9], already known, and brown crystals of $K_6(VO)_2(V_2O_3)_2(PO_4)_4(P_2O_7)$. For the latter phosphate two crystals were selected for the structure determination, whose volumes differ by one order of magnitude (Table 1).

1.2. Structure solution on a small crystal: average structure in the Pnma subcell

The data collected on the first crystal with a CCD camera show an orthorhombic cell, $a = 6.9801(9)$ Å, $b = 13.3889(34)$ Å, $c = 14.2342(17)$ Å, with systematic extinction compatible with the *Pnma* or $Pn2_1a$ space groups. Based on our previous study of the Rb-phase $Rb_6(VO)_2(V_2O_3)_2(PO_4)_4(P_2O_7)$ [4], we solved the structure of our K-phosphate in the *Pnma* space group, using the atomic parameters of the Rb-phosphate as starting parameters. The least squares refinements of the atomic co-ordinates and their anisotropic thermal parameters performed on the

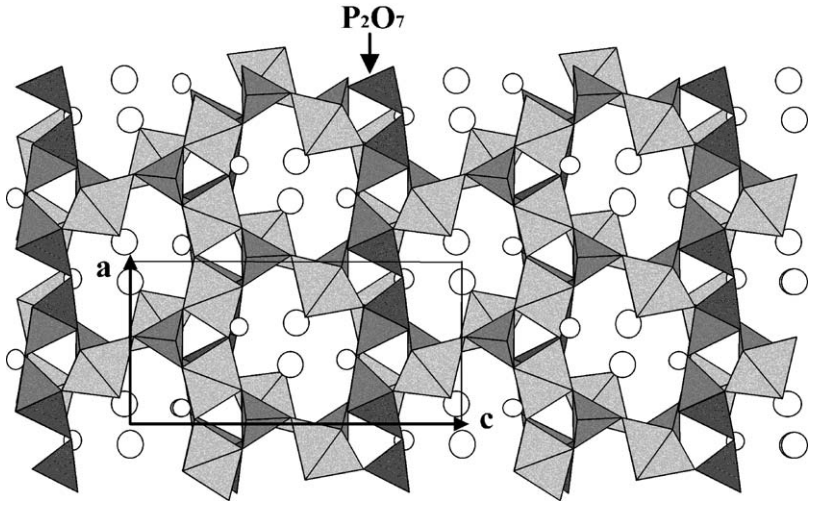

Fig. 1. Projection along $\vec{b}$ of the average structure of $K_6(VO)_2(V_2O_3)_2(PO_4)_4(P_2O_7)$ in the *Pnma* subcell. Two levels of gray distinguish the two neighboring sites of P_2O_7.

F^2 corrected for absorption phenomena, lead to $R = 4.67\%$ and $R_w = 3.17\%$.

The so obtained framework (Fig. 1) is the same as that observed for $Rb_6(VO)_2(V_2O_3)_2(PO_4)_4(P_2O_7)$. It is especially characterized by P_2O_7 groups distributed at random over two sites. Thus from such a crystal, no additional reflections can be observed with respect to the Rb-phosphate and the ordering of the P_2O_7 groups if it exists should be considered in this subcell, with a different space group. The $Pnm2_1$ space group (other setting of the $Pmn2_1$ space group no. 31) answers this condition. The $h = 2n + 1$ systematic extinction in $hk0$ is indeed induced by pairs of atoms of coordinates x, y, z and $x + 1/2$, y, z' without any relation between z and z'.

We could then set up a similar structure in this group, characterized by an ordering of the P_2O_7 groups. The refinements allowed the reliability factors to be lowered to $R = 5.63\%$ and $R_w = 4.12\%$, but the difference Fourier maps showed that there exist high peaks corresponding to the occupancy of a second site by the P_2O_7 groups.

At this point, it can be stated that such a subcell implies in any case disordering of the P_2O_7 groups. Consequently, an ordering of the P_2O_7 groups if it exists should give rise to a larger cell, characterized by very weak additional reflections. The latter may not be detected, due to the too small size of the crystal.

Table 2
P–O distances in the supercell

*P*1*a*–O3^{ii}	1.568(6) Å	*P*1*e*–O2^{iii}	1.507(6) Å
*P*1*a*–O21^{iii}	1.568(8)	*P*1*e*–O20^{ii}	1.521(6)
*P*1*a*–O41	1.528(6)	*P*1*e*–O48^{ii}	1.507(6)
*P*1*a*–O44^{ii}	1.528(6)	*P*1*e*–O56	1.534(8)
*P*1*b*–O11^{iv}	1.574(6) Å	*P*1*f*–O12^{vi}	1.560(6) Å
*P*1*b*–O30	1.500(6)	*P*1*f*–O29^{vii}	1.503(6)
*P*1*b*–O39	1.527(6)	*P*1*f*–O51	1.515(6)
*P*1*b*–O45	1.533(6)	*P*1*f*–O53	1.513(6)
*P*1*c*–O7^{ii}	1.559(6) Å	*P*1*g*–O25^{vii}	1.558(6) Å
*P*1*c*–O8^{iv}	1.543(6)	*P*1*g*–O26^{ii}	1.526(6)
*P*1*c*–O40	1.508(6)	*P*1*g*–O49^{ii}	1.517(6)
*P*1*c*–O43^{ii}	1.515(6)	*P*1*g*–O55	1.554(6)
*P*1*d*–O34^{v}	1.563(6) Å	*P*1*h*–O16^{vi}	1.532(6) Å
*P*1*d*–O35	1.546(6)	*P*1*h*–O17^{v}	1.505(6)
*P*1*d*–O38	1.496(6)	*P*1*h*–O50	1.525(7)
*P*1*d*–O46	1.536(6)	*P*1*h*–O54	1.550(6)
*P*2*a*–O4	1.550(8) Å	*P*3*a*–O13	1.507(6) Å
*P*2*a*–O9	1.508(6)	*P*3*a*–O18	1.512(6)
*P*2*a*–O57	1.643(6)	*P*3*a*–O57	1.611(7)
*P*2*a*–O59	1.489(6)	*P*3*a*–O62	1.479(8)
*P*2*b*–O31	1.550(8) Å	*P*3*b*–O22^{ii}	1.523(6) Å
*P*2*b*–O36	1.512(8)	*P*3*b*–O27^{ii}	1.543(8)
*P*2*b*–O58	1.646(7)	*P*3*b*–O58	1.605(7)
*P*2*b*–O60	1.526(6)	*P*3*b*–O61	1.491(7)

The symmetry codes are put at the end of Table 4.

1.3. Structure solution on a large crystal: the actual structure

The data collected with a second crystal, ten times larger than the first one, evidence more than 4000 additional independent reflections, leading to the supercell $a = 26.7777$ Å, $b = 28.480$ Å, $c = 6.9762$ Å, $\alpha = \beta = \gamma = 90^\circ$ with a C centering (Table 1).

All the strong reflections belong to the orthorhombic subcell and the additional reflections creating the supercell are weak. Moreover, the differences between the values of the intensities do not allow to differentiate the dispersion of the measurements from a possible lowering of the symmetry. It results in a great difficulty for choosing the space group of the supercell for the structure resolution. Thus, our choice was only based on the interest of finding out an eventual ordering of the P_2O_7 groups in this supercell, bearing in mind that the general feature of the subcell must be maintained. Considering the whole framework, but without the P_2O_7 groups, according to the results obtained for the subcell, no mirror plane or twofold axis may exist perpendicular to the c-axis, and similarly no mirror plane perpendicular to the b-axis.

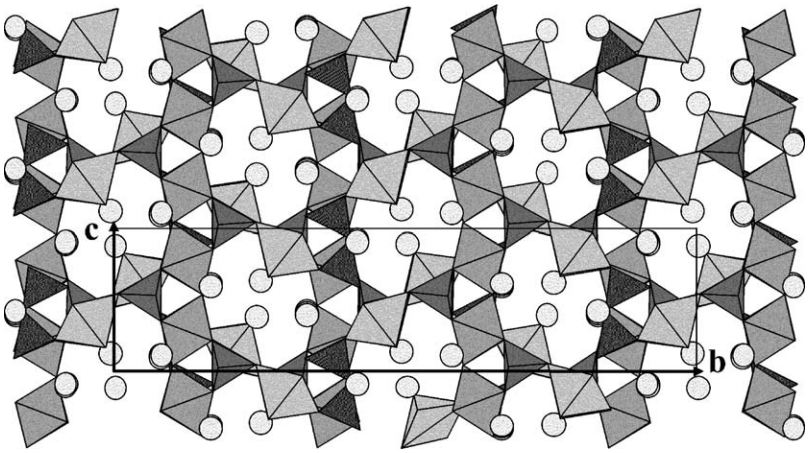

Fig. 2. (a) Partial projection along $\vec{a}$ of the actual structure of $K_6(VO)_2(V_2O_3)_2(PO_4)_4(P_2O_7)$ in the C-1 supercell. (b) Partial projection along $\vec{b}$ showing the ordering of the P_2O_7 units (in dark gray).

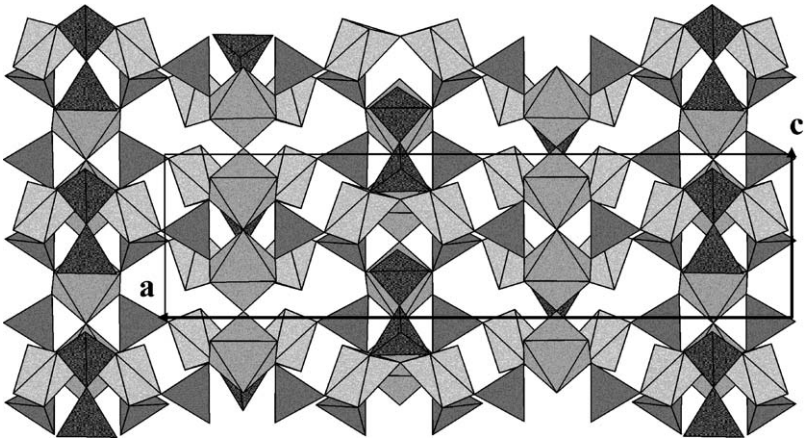

Fig. 2. (*Continued*)

Based on the above considerations, and taking into account the systematic absences observed in the reciprocal space, only one space group with the orthorhombic symmetry, $Cmc2_1$, is available. The latter regenerates correctly the framework, but does not suppress the disordering of the P_2O_7 groups in the structure. Since no orthorhombic space group allows an ordering of the P_2O_7 groups, the monoclinic symmetry was explored. We found out the possible $Cm11$ space group, admitting that the differences between the intensity values of the superstructure reflections are significant. In this space group, an ordering of the P_2O_7 groups can be built, without the $b/2$ translation in the true mirrors but with this translation in the glide planes sitting between the mirrors. In this model, the refinement of the atomic parameters does not converge and the difference Fourier maps show high peaks corresponding to a second site for the P_2O_7 groups, located in the b glide planes between the mirrors. Finally the symmetry was lowered to the triclinic space group C-1. In this group, the center of symmetry sits at same place as in the orthorhombic subcell. To correctly perform the refinements without high correlation between the parts which are related in the subcell, we used a unitary weight, so the very weak supercell reflections may influence it. The refinements work very well and lead to $R = 5.06\%$ and $R_w = 5.12\%$. This refinement definitely demonstrates clearly the ordering of the diphosphate groups, as it will be further discussed (Table 2).

Table 3
V–O distances in the supercell

V1*a*–O1	1.588(7) Å	V1*e*–O19	1.608(6) Å
V1*a*–O2	1.990(6)	V1*e*–O20	1.971(6)
V1*a*–O3	1.926(7)	V1*e*–O21	1.985(7)
V1*a*–O4	2.011(6)	V1*e*–O22	2.023(6)
V1*a*–O5	1.787(6)	V1*e*–O23	1.840(6)
V1*a*–O62^{i}	2.631(8)	V1*e*–O60^{i}	2.633(7)
V1*b*–O5	1.825(6) Å	V1*f*–O23	1.782(6) Å
V1*b*–O6	1.627(7)	V1*f*–O24	1.593(7)
V1*b*–O7	1.943(6)	V1*f*–O25	2.003(6)
V1*b*–O8	1.957(6)	V1*f*–O26	1.945(6)
V1*b*–O9	2.018(6)	V1*f*–O27	2.025(8)
V1*b*–O62^{i}	2.587(8)	V1*f*–O60^{i}	2.697(7)
V1*c*–O10	1.583(7) Å	V1*g*–O28	1.642(7) Å
V1*c*–O11	1.957(6)	V1*g*–O29	2.019(6)
V1*c*–O12	1.942(6)	V1*g*–O30	1.964(6)
V1*c*–O13	2.033(6)	V1*g*–O31	2.024(6)
V1*c*–O14	1.767(8)	V1*g*–O32	1.843(6)
V1*c*–O59	2.782(7)	V1*g*–O61^{i}	2.522(7)
V1*d*–O14	1.854(8) Å	V1*h*–O32	1.782(6) Å
V1*d*–O15	1.603(7)	V1*h*–O33	1.585(8)
V1*d*–O16	1.941(6)	V1*h*–O34	1.988(6)
V1*d*–O17	1.987(6)	V1*h*–O35	1.966(7)
V1*d*–O18	2.021(6)	V1*h*–O36	2.032(6)
V1*d*–O59	2.611(7)	V1*h*–O61^{i}	2.680(7)
V2*a*–O37	1.624(6) Å	V2*c*–O47	1.629(6) Å
V2*a*–O38	1.951(6)	V2*c*–O48	1.959(6)
V2*a*–O39	1.979(6)	V2*c*–O49	1.983(6)
V2*a*–O40	2.017(6)	V2*c*–O50	2.017(7)
V2*a*–O41	1.997(6)	V2*c*–O51	2.022(6)
V2*a*–O42	2.136(6)	V2*c*–O52	2.148(6)
V2*b*–O37^{i}	2.163(6) Å	V2*d*–O47	2.167(6) Å
V2*b*–O42	1.639(6)	V2*d*–O52^{ii}	1.625(6)
V2*b*–O43	1.939(6)	V2*d*–O53	1.937(6)
V2*b*–O44	1.946(6)	V2*d*–O54	1.949(6)
V2*b*–O45	2.003(6)	V2*d*–O55	1.989(6)
V2*b*–O46	1.994(6)	V2*d*–O56	1.998(8)

The symmetry codes are put at the end of Table 4.

2. Discussion

The partial projections of the actual structural along $\vec{a}$ (Fig. 2a) and $\vec{b}$ (Fig. 2b) show that a great majority of polyhedra keep the orthorhombic symmetry of the subcell. The 3D-framework $[V_6P_6O_{31}]_\infty$ is built up of octahedral $[VO_5]_\infty$ chains running along $\vec{c}$, assembled with $[V_2P_2O_{13}]_\infty$ double chains running along $\vec{a}$ and involving single PO_4 tetrahedra and double pyramidal units V_2O_9. In this structure, only the P atoms of the P_2O_7 groups (*P*2*a*, *P*2*b*, *P*3*a*, *P*3*b*) and the oxygen atoms bridging the two phosphorus atoms of the P_2O_7 groups (O57, O58) are responsible for the weak extra reflections, and imply a doubling of the a and b parameters. As a consequence, the P_2O_7 groups are really ordered, and in contrast to the rest

of atoms of the structure, they are not related by a $b/2$ or $a/2$ translation (or pseudo-translations). Thus two successive rows of P_2O_7 groups running along $\vec{c}$ that are spaced by $a/2$ or $b/2$ do not exhibit the same orientation of their disphosphate groups.

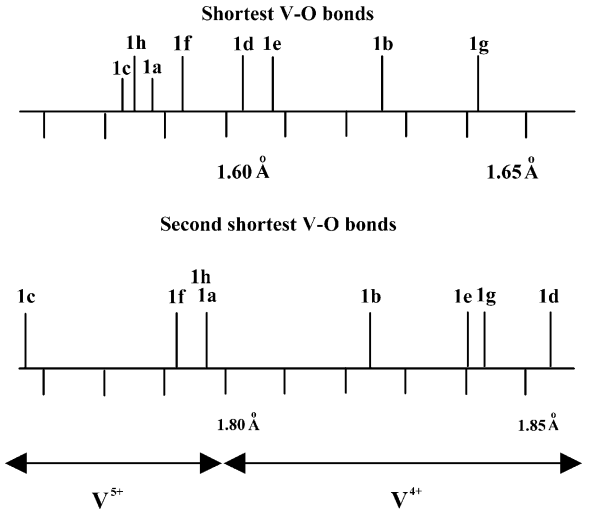

Fig. 3. The distribution of the length of the shortest and second shortest V–O bonds in the V1**O_5 pyramids.

Similarly, the geometry of the VO_5 pyramids (labeled V1**) forming the V_2O_9 units is different from that described in the subcell: two VO_5 pyramids belonging to the same V_2O_9 unit are no more identical, and in the same way two VO_5 pyramids spaced by $a/2$ are no more identical. This means that, due to the different orientation of the successive rows of P_2O_7 groups, two kinds of V1** pyramids must be distinguished as shown from Table 3 and Fig. 3. In the first group—V1*a*, V1*c*, V1*f* and V1*h*—the pyramids exhibit a "vanadyl" bond shorter than 1.60 Å (1.583–1.593 Å), one intermediate (1.767–1.787 Å) and three larger ones (1.926–2.033 Å), the sixth distance being much longer (2.631–2.782 Å). In the second group—V1*b*, V1*d*, V1*e*, V1*g*—the "vanadyl" bond is longer than 1.60 Å (1.603–1.642 Å) and one observes four longer basal bonds (1.825–2.024 Å), the sixth distance ranging from 2.522 to 2.633 Å. In contrast, the V–O distances, characterizing the VO_6 octahedra (labeled V2**) are not changed with respect to the subcell: one observes a short vanadyl V–O bond (1.624–1.639 Å) opposed to a longer one (2.136–2.167 Å)

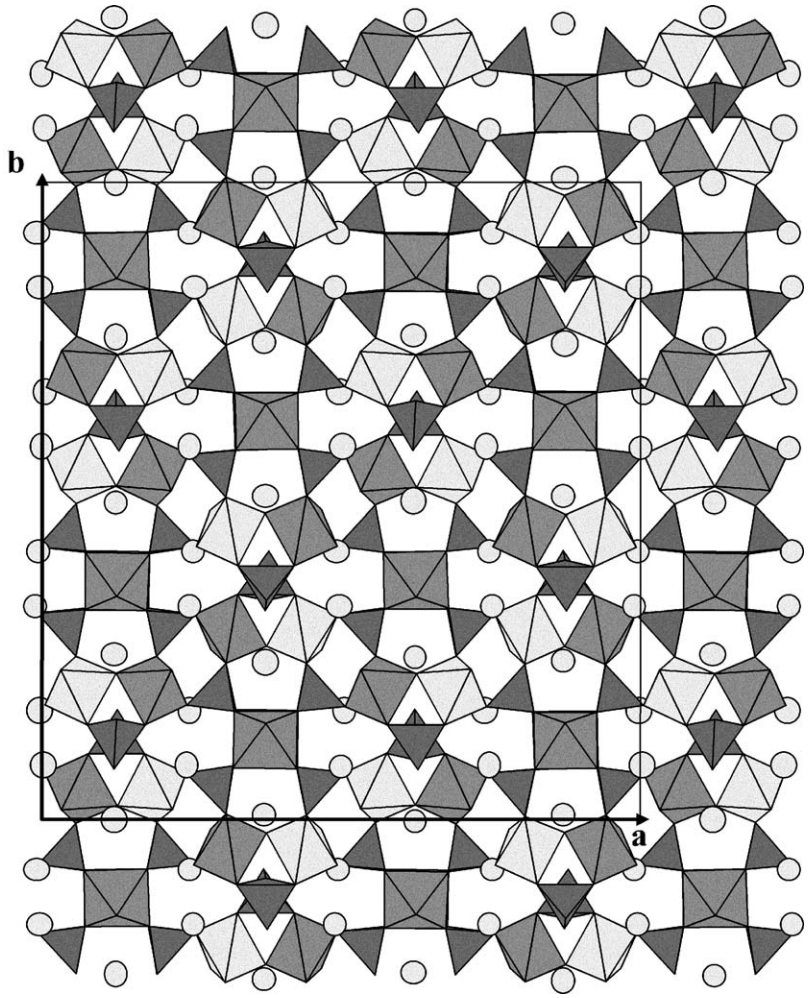

Fig. 4. Projection along $\vec{c}$ of the actual structure of $K_6(VO)_2(V_2O_3)_2(PO_4)_4(P_2O_7)$ showing the ordering of the V^{5+} (light gray) and of the V^{4+} (medium gray) species through the frameworks.

Table 4
K–O distances in the supercell

K1*a*–O54^{iii}	2.715(6)	K1*a*–O17	3.010(7)
K1*a*–O2	2.785(6)	K1*a*–O18^{i}	3.021(7)
K1*a*–O15^{ii}	2.786(7)	K1*a*–O56^{iii}	3.313(9)
K1*a*–O4	2.877(7)	K1*a*–O50^{iii}	3.349(8)
K1*a*–O15^{iii}	2.989(7)		
K1*b*–O43^{iv}	2.734(6)	K1*b*–O13	3.072(6)
K1*b*–O6	2.774(7)	K1*b*–O9	3.115(6)
K1*b*–O11	2.775(6)	K1*b*–O45^{iv}	3.202(6)
K1*b*–O6^{iv}	2.964(6)	K1*b*–O40^{iv}	3.305(7)
K1*b*–O8^{i}	3.003(7)	K1*b*–O57	3.340(6)
K1*c*–O39^{iv}	2.689(6)	K1*c*–O28^{iv}	3.004(7)
K1*c*–O10^{i}	2.788(7)	K1*c*–O13^{i}	3.013(7)
K1*c*–O8	2.810(6)	K1*c*–O40^{iv}	3.348(6)
K1*c*–O9	2.881(6)	K1*c*–O45^{v}	3.398(6)
K1*c*–O11	2.988(7)		
K1*d*–O48^{viii}	2.692(6)	K1*d*–O18^{v}	3.097(6)
K1*d*–O1^{iv}	2.784(7)	K1*d*–O4^{v}	3.106(8)
K1*d*–O17^{iv}	2.796(6)	K1*d*–O56^{ix}	3.252(8)
K1*d*–O19^{ix}	2.939(6)	K1*d*–O50^{ix}	3.262(7)
K1*d*–O2^{v}	3.058(6)	K1*d*–O57^{iv}	3.348(6)
K1*e*–O38^{iv}	2.713(6)	K1*e*–O22^{ix}	3.071(6)
K1*e*–O21^{ix}	2.770(6)	K1*e*–O36^{x}	3.110(8)
K1*e*–O33^{x}	2.790(8)	K1*e*–O41^{iv}	3.322(6)
K1*e*–O33^{iv}	2.939(9)	K1*e*–O46^{v}	3.331(7)
K1*e*–O34^{ix}	2.989(7)	K1*e*–O58^{x}	3.334(8)
K1*f*–O49^{ix}	2.717(6)	K1*f*–O27^{xi}	2.965(8)
K1*f*–O24^{xi}	2.776(7)	K1*f*–O24^{ix}	2.994(7)
K1*f*–O29^{xi}	2.783(6)	K1*f*–O25^{xii}	3.004(7)
K1*f*–O31^{xi}	2.841(7)		
K1*g*–O53^{vii}	2.734(6)	K1*g*–O27	3.083(8)
K1*g*–O25	2.751(6)	K1*g*–O31^{i}	3.091(8)
K1*g*–O28^{i}	2.756(7)	K1*g*–O51^{xiii}	3.289(7)
K1*g*–O10^{iv}	2.939(6)	K1*g*–O55^{xiii}	3.296(6)
K1*g*–O29	3.013(7)	K1*g*–O58^{i}	3.334(8)
K1*h*–O44^{viii}	2.760(6)	K1*h*–O21^{xiii}	2.958(8)
K1*h*–O34^{vii}	2.765(6)	K1*h*–O22^{vii}	2.998(7)
K1*h*–O19^{vii}	2.780(7)	K1*h*–O1^{viii}	3.029(7)
K1*h*–O36^{vii}	2.846(7)	K1*h*–O46^{viii}	3.360(6)
K2*a*–O58^{i}	2.825(6)	K2*a*–O30	2.900(6)
K2*a*–O46	2.827(6)	K2*a*–O35	2.914(8)
K2*a*–O32^{i}	2.867(6)	K2*a*–O61^{i}	3.134(7)
K2*a*–O45	2.875(6)	K2*a*–O28^{i}	3.205(8)
K2*a*–O37^{i}	2.898(6)	K2*a*–O33^{i}	3.268(8)
K2*b*–O41^{iv}	2.774(6)	K2*b*–O3^{v}	2.907(8)
K2*b*–O40^{iv}	2.824(6)	K2*b*–O7^{v}	2.935(6)
K2*b*–O57^{iv}	2.836(6)	K2*b*–O62^{iv}	3.154(8)
K2*b*–O5^{iv}	2.869(7)	K2*b*–O6^{iv}	3.243(6)
K2*b*–O42^{iv}	2.894(6)	K2*b*–O1^{iv}	3.262(8)
K2*c*–O51	2.755(6)^{ix}	K2*c*–O52^{ix}	2.971(6)
K2*c*–O50	2.822(7)^{ix}	K2*c*–O59^{viii}	3.044(7)
K2*c*–O14	2.895(7)^{xiv}	K2*c*–O15^{xiv}	3.238(8)
K2*c*–O12	2.912(7)^{viii}	K2*c*–O10^{xiv}	3.302(8)
K2*c*–O16	2.913(6)^{viii}		
K2*d*–O55^{xi}	2.804(6)	K2*d*–O47^{xi}	2.966(6)
K2*d*–O26^{xii}	2.867(6)	K2*d*–O60^{xi}	2.997(7)
K2*d*–O56^{xi}	2.869(9)	K2*d*–O24^{xi}	3.250(8)
K2*d*–O23^{xi}	2.884(6)	K2*d*–O19^{xi}	3.259(6)
K2*d*–O20^{xii}	2.904(6)		

Symmetry codes
i: $x, y, z-1$; ii: $x, y, z+1$; iii: $-x, 1-y, 1-z$; iv: $1/2-x, 1/2-y, 1-z$; v: $1/2-x, 1/2-y, -z$; vi: $x, 1+y, z$; vii: $1/2-x, 1.5-y, 1-z$; viii: $1/2+x, 1/2+y, z$; ix: $1/2+x, y-1/2, z$; x: $1/2+x, y-1/2, z-1$; xi: $1-x, 1-y, 1-z$; xii: $1-x, 1-y, -z$; xiii: $1/2-x, 1.5-y, -z$; xiv: $1/2+x, 1/2+y, z-1$.

and four intermediate V–O distances (1.937–2.022 Å). At this point, the calculations of bond valence sums are of great interest, in order to detect a possible charge ordering in the vanadium network. Starting from the R_{ij} values given by Brese and O'Keeffe [10] one observes that the V2** octahedra and the V1** pyramids of the second group (V1*b*, V1*d*, V1*e*, V1*g*) have the same valences close to 4.30, whereas the V1 pyramids of the first groups (V1a, V1c, V1f, V1h) exhibit a significantly higher valence close to 4.80. This strongly suggests that the V2** octahedra and V1** pyramids of the second group are occupied by V^{4+} species, whereas the V^{5+} species sit in the first group of V1** pyramids. The geometry of the V^{5+} pyramids described previously by Boudin et al. [11] is in perfect agreement with that observed for the first group of V1** pyramids. Using different values of R_{ij}, i.e. $R_{ij} = 1.7609$ for V^{4+} and $R_{ij} = 1.8188$ for V^{5+}, in the bond valence calculations one obtains valences ranging from 3.87 to 4.083 for V2** and V1** (2nd group) and from 4.931 to 5.083 for V1** (1st group). Thus, concomitant to the ordering of the P_2O_7 groups one observes a very regular charge ordering of the vanadium species in perfect agreement with the chemical formula which implies a V^{4+}/V^{5+} molar ratio equal to 2:1. The projection of the structure along $\vec{c}$ (Fig. 4) shows that the rows of VO_6 octahedra are tetravalent, whereas around each P_2O_7 group, the two V_2O_9 units form "V^{4+}–V^{5+}" pairs. As a result, the V^{4+} and V^{5+} species form stripes running along the [110] direction, according to the sequence "$V2^{4+}$–$V1^{5+}$–$V1^{4+}$–$V1^{4+}$–$V1^{5+}$–$V2^{4+}$" or to the sequence "$V2^{4+}$–$V1^{4+}$–$V1^{5+}$–$V1^{5+}$–$V1^{4+}$–$V2^{4+}$" for the adjacent stripe.

Finally, the ordered distribution of the P_2O_7 groups, and more exactly of the O57 and O58 atoms leads to a change of the coordination of potassium with respect to the subcell. The latter ranges from 7 to 10 for the K1** species and from 9 to 10 for the K2** species instead of 10 in the subcell (Table 4).

In conclusion, the structural study of $K_6(VO)_2(V_2O_3)_2(PO_4)_4(P_2O_7)$, using larger single crystals than previously, and registering the reciprocal space with a CCD camera, has allowed the actual structure of this phase to be solved, showing an ordering of the P_2O_7 groups and concomitantly an ordering of the charges on the vanadium species. It is most probable that other members of this series $A_6(V_2O_3)_2(VO)_2(PO_4)_4$ $(H_yP_{2-x}V_xO_7)$ with $A = K$, Rb, Tl, exhibit similar ordering phenomena since the resolution of such actual structures is strongly sensitive to both, the size of the investigated crystal and the detection method.

References

[1] P. Roussel, O. Perez, Ph. Labbé, Acta Crystallogr. B 57 (2001) 603–632.
[2] A. Rötger, J. Lehmann, C. Schlenker, J. Dumas, J. Marcus, Z.S. Teweldemedhin, M. Greenblatt, Europhys. Lett. 25 (1) (1994) 23–29.
[3] M.M. Borel, A. Leclaire, J. Chardon, B. Raveau, J. Mater. Chem. 8 (3) (1998) 693–697.

[4] L. Benhamada, A. Grandin, M.M. Borel, A. Leclaire, B. Raveau, J. Solid State Chem. 94 (1991) 274–280.
[5] E. Le Fur, B. de Villars, J. Tortelier, J.Y. Pivan, Int. J. Inorg. Mater. 3 (2001) 341–345.
[6] E. Le Fur, B. de Villars, J. Tortelier, J.Y. Pivan, Int. J. Inorg. Mater. 3 (2001) 9–15.
[7] G. Costentin, A. Leclaire, M.M. Borel, A. Grandin, B. Raveau, Z. Kristallogr. 201 (1992) 53–58.
[8] S.E. Lister, I.R. Evans, J.A.K. Howard, A. Coelho, J.S.O. Evans, Chem. Commun. 22 (2004) 2540–2541.
[9] Y.E. Gorbunava, S.A. Linde, A.V. Lavrov, I.V. Tananaev, Dokl. Akad. Nauk SSSR 250 (1980) 350–353.
[10] N.E. Brese, M. O'Keeffe, Acta Crystallogr. B 47 (1991) 192–197.
[11] S. Boudin, A. Guesdon, A. Leclaire, M.M. Borel, Int. J. Inorg. Mater. 2 (2000) 561–579.